Carbohydrate Polymers 88 (2012) 604–608

Contents lists available at SciVerse ScienceDirect

Carbohydrate Polymers

journal homepage: www.elsevier.com/locate/carbpol

Preparation and properties of the succinic ester of porous starch

Peter R. Chang[b,*], Dayan Qian[a], Debbie P. Anderson[b], Xiaofei Ma[a,**]

[a] Chemistry Department, School of Science, Tianjin University, Tianjin 300072, China
[b] Bioproducts and Bioprocesses National Science Program, Agriculture and Agri-Food Canada, 107 Science Place, Saskatoon, SK S7N 0X2, Canada

ARTICLE INFO

Article history:
Received 4 December 2011
Received in revised form
22 December 2011
Accepted 1 January 2012
Available online 8 January 2012

Keywords:
Porous starch
Succinic anhydride
Adsorption

ABSTRACT

Porous starch (PS) was prepared by replacing ice crystals in frozen starch gel with ethanol using a solvent exchange technique. It was then modified by succinic anhydride (SA) in a solvent/catalyst-free medium, and the obtained SA-modified PSs (SAPSs) were characterized. The degrees of substitution (DSs) of SA could be controlled by changing the SA/starch molar ratios. A high linear relationship (>0.99) between the DS and molar ratio was found. The effect of different DSs (0–1.90) on the pore size, apparent density, moisture adsorption, oil adsorption capacity and methylene blue (MB) adsorption of SAPSs was investigated. Apparent density, oil adsorption capacity and methylene blue (MB) adsorption of SAPSs increased gradually with the increasing DSs. SAPSs exhibited higher moisture content at equilibrium than PS. In addition, the adsorption of MB by SAPSs could be described well by a pseudo second-order model.

1. Introduction

Starch is abundant, renewable, inexpensive, biodegradable, and environmentally friendly, making it one of the most attractive and promising bioresources for industrial applications. Chemical modification is a powerful tool widely used for improving the properties of starch in order to meet specific requirements of some applications. These modifications disrupt the hydrogen bonding and reduce retrogradation while imparting special features/functionalities, e.g. hydrophobicity, to the native starch (Bhosale & Singhal, 2006). Since native starch commonly exists in a granular structure with about 15–45% crystallinity, these modifications usually require caustic conditions for a high degree of substitution. Octenyl succinic anhydride (OSA) modified starch is produced by esterification of native starch with octenyl succinic anhydride. The reaction can reach a higher DS (1.21) using pyridine (Wang et al., 2011) as the solvent/catalyst than aqueous NaOH solution (0.022) as the solvent (Bhosale & Singhal, 2006). Yoshimura, Yoshimura, Seki, and Fujioka (2006) reported the reaction of starch and succinic anhydride (SA) ($0.4 < DS < 1.4$), using 4-dimethylaminopyridine as the esterification catalyst and dimethylsulfoxide (DMSO) as the solvent. Generally, starch esters are prepared under high temperature, pressure, and intensive mixing conditions in order to achieve a desirable reaction levels with the esterification reagent. For example, starch acetates of DS 0.5–2.5 were prepared at temperatures of 160–180 °C (Shogren, 2003). Similarly, the maximum transesterification of amylomaize starch (DS = 0.61) was obtained after 4.5 h at 190 °C (Aburto, Alric, & Borredon, 2005). Most commercially available starch esters, i.e. starch acetates, alkenyl-succinates, phosphates and adipates, usually have low DS (<0.1), and they are used either in suspend or soluble form for food applications (Shogren, 2003).

Porous starch (PS) is an economical and biodegradable adsorbent that has been widely used in food, pharmaceuticals, agriculture, cosmetics, pulp and paper, and other industries (Qian, Chang, & Ma, 2011). Currently, a freezing-solvent exchange technique has been used to prepare PS by replacing ice crystals in frozen starch gel with the mixed solvent of ethanol and water. The size of the holes in PS was variable with ethanol/water ratios (Chang, Yu, & Ma, 2011). In addition, porosity of PS can be easily manipulated by adjusting starch paste concentrations and the number of freezing cycles (Qian et al., 2011). Presumably, large specific surface area of PS would make chemical modification (e.g. esterification) more effectively. Hence, in this work, succinic anhydride (SA) was used to further modify PS previously prepared using a freezing-solvent exchange technique at 110 °C for 4 h in a solvent/catalyst-free medium. The dependence of DSs and reaction efficiencies on SA/starch molar ratios was investigated. And the effects of the SA modification on the pore structure, apparent densities, moisture adsorption, oil adsorption and dye adsorption of SA-modified PSs (SAPSs) are discussed.

* Corresponding author.
** Corresponding author. Tel.: +86 22 27406144; fax: +86 22 27403475.
E-mail addresses: peter.chang@agr.gc.ca (P.R. Chang), maxiaofei@tju.edu.cn (X. Ma).

0144-8617/$ – see front matter. Crown Copyright © 2012 Published by Elsevier Ltd. All rights reserved.
doi:10.1016/j.carbpol.2012.01.001

2. Materials and methods

2.1. Materials

Potato starch was supplied by Manitoba Starch Products (Manitoba, Canada). Soybean oil was produced by COFCO Northsea Oils & Grains (Tianjin) Co. Ltd., China. The methylene blue (MB) dye was provided by Tianjin Benchmark Chemical Reagent Co. Ltd., China. Ethanol, acetone and succinic anhydride (SA) were analytical reagents purchased from Tianjin Chemical Reagent Factory, China.

2.2. Preparation of PS in the freezing process

The preparation of PS was based on the method of Chang et al. (2011). Potato starch (10 g) was added into 200 mL of distilled water. The mixture was heated at 90 °C for 0.5 h for complete gelatinization of the starch. It was then cooled at 5 °C to obtain starch gel. The gel was cut into cubes (about 1 cm × 1 cm × 1 cm), and frozen at −10 °C. The frozen cubes were immersed in ethanol at room temperature. The cubes were immersed three times, for about 1 h each time, in ethanol. The cubes were dried at 50 °C for 6 h to remove the ethanol and to obtain white, solid PS cubes.

2.3. Preparation of SA-modified PSs (SAPSs)

SA modification was based on the method of Ma, Chang, Yu, and Stumborg (2009b) with some modifications. SA was dissolved in acetone. The PS cubes were immersed in acetone solution with the different SA concentrations to completely absorb it and then conditioned for 12 h at room temperature. The molar ratios of SA and PS were 0.3, 0.6, 0.9, 1.2 and 1.5, respectively. The molar mass of starch (i.e. anhydroglucose unit) of 162 was used to design the above variables. They were subsequently dried and reacted at 110 °C for 4 h in a forced air oven. SA-modified PS (SAPS) was immersed in ethanol and washed three times to remove the remnant SA, and then dried and used for testing.

2.4. Determination of the molar degree of substitution by SA

Molar degree of substitution (DS) is the average number of hydroxyl groups substituted per anhydroglucose unit of starch. DS was determined using the method of Ma, Jian, Chang, and Yu (2008) with minor modifications. SAPS was ground to a powder prior to the testing of DS, and approximately 1.0 g of dry SAPS powder was accurately weighed and placed into a 250 mL conical flask. Then 50 mL of 75% ethanol solution was added and the conical flask was agitated and warmed at 50 °C for 1 h before cooling to room temperature. Standard 0.500 M aqueous sodium hydroxide solution (20 mL) was added; the conical flask was tightly stoppered, and saponified at 30 °C with a magnetic stirrer for 24 h. The excess alkali was back-titrated with a standard 0.200 M aqueous hydrochloric acid solution and re-titrated 2 h later to account for any further alkali that may have leached from the starch.

DS was calculated by using following equations (Bai & Shi, 2011):

$$\%SA = \frac{(V_1 - V_2) \times 10^{-3} \times C_{HCl} \times 100}{m} \quad (1)$$

$$DS = \frac{162 \times \%SA}{100 - 99 \times \%SA} \quad (2)$$

where V_1, volume (mL) of HCl required for blank titration; V_2, volume (mL) of HCl required for sample titration; m, weight of sample taken (g); C_{HCl}, the concentration of HCl solution; 162 = the molar mass of starch (i.e. anhydroglucose unit); 100 = molecular weight of SA. Reaction efficiencies (REs) were calculated as the ratio of measured DS to the molar ratio of SA/starch (Shogren, 2003).

2.5. Fourier transform infrared spectroscopy (FTIR)

FTIR spectroscopy of SAPS powders was performed at 2 cm^{-1} resolution with a BIO-RAD FTS3000 IR Spectrum Scanner. Samples were prepared by making pellets with dried IR grade KBr and typically 64 scans were signal-averaged to reduce spectral noise.

2.6. Scanning electron microscopy (SEM)

The fracture surfaces of SAPS were examined using a Philips XL-3 scanning electron microscope. SAPS was cooled in liquid nitrogen and then broken. The fracture surfaces of SAPSs were vacuum coated with gold for SEM.

2.7. Apparent density

The apparent density of SAPSs, also called bulk density, was defined as the mass of material divided by the total volume it occupies (Wong, Chu, Leung, Park, & Zong, 2011). The data were averaged from 5 cubes.

2.8. Moisture adsorption

Dried SAPS cubes were stored in a closed chamber with a relative humidity (RH) of 75% at 20 °C for a period of time. The moistures in the SAPS cubes were calculated based on the final weight (w) and original weight (w_0) as follows:

$$\text{Moisture content (wt\%)} = \left(\frac{w}{w_0} - 1\right) \times 100 \quad (3)$$

2.9. Oil adsorption capacity

The dried SAPS cubes (weight = w_0) were immersed in soybean oil for 0.5 h at room temperature with constant stirring. The mixture was filtered in a funnel under gravity. When there was no more oil dripping from the filter paper, SAPS was weighed (w). The oil adsorption capacity was calculated as follow:

$$\text{Oil adsorption capacity} = \frac{w - w_0}{w_0} \quad (4)$$

2.10. Adsorption experiments

Adsorption experiments were conducted using glass bottles containing 10 g L^{-1} of SAPS and 0.0854 mmol L^{-1} (31.93 mg L^{-1}) MB dye. The glass bottles were placed on a slow-moving platform shaker and aliquots of approximately 10 mL were taken at different time intervals during the reaction. The MB dye concentration in the solution was analyzed by UV–Vis spectrometry and relative dye adsorption versus reaction time determined.

3. Results and discussion

3.1. The effect of SA/starch ratio on the reaction

The dependence of DS and RE on SA/starch molar ratio is shown in Fig. 1. A linear increase in the DS of the SA PS was observed with an increase in the SA/starch ratio. The linear equation with a high correlation coefficient ($R > 0.99$) is expressed as $y = 0.0224 + 1.3099x$. The symbols x and y represent the SA/starch molar ratio and DS, respectively. The increase in DS with the increase in SA/starch ratio could be interpreted in terms of the greater availability of the SA molecules in the proximity of the starch molecule. It is well known that starch hydroxyls are immobile and their reaction will therefore rely on the availability of SA molecules in the vicinity of the hydroxyl groups. Similar results

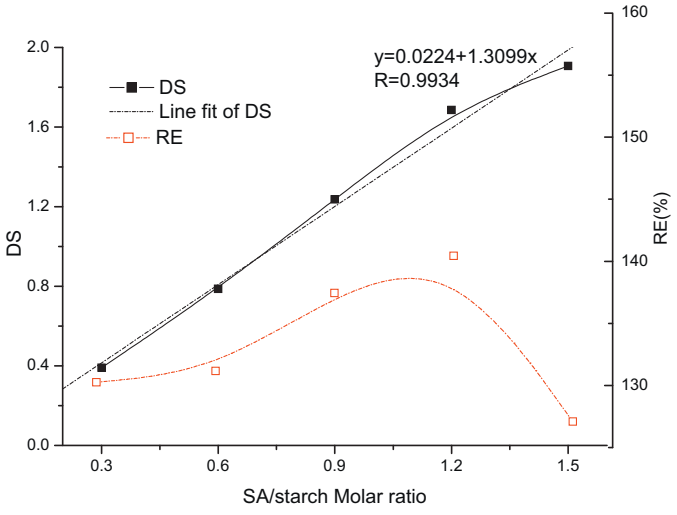

Fig. 1. Effect of SA/starch molar ratios on the DSs and REs of SAPSs.

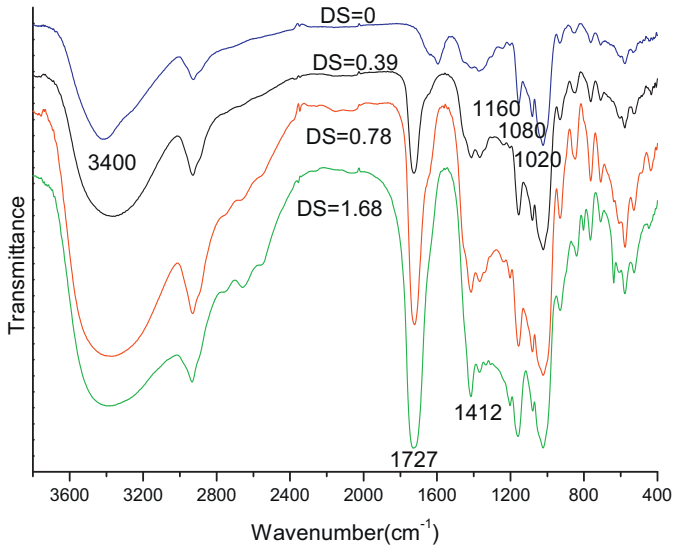

Fig. 2. FTIR of spectra of PS and SAPSs with different DSs.

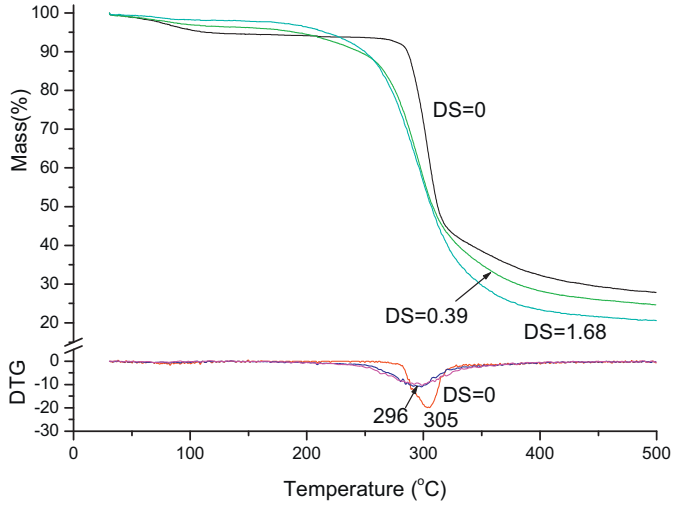

Fig. 3. Thermogravimetric (TG) and derivative thermogravimetric (DTG) curves of PS and SAPSs with different DSs (DS = 0.39 and 1.68).

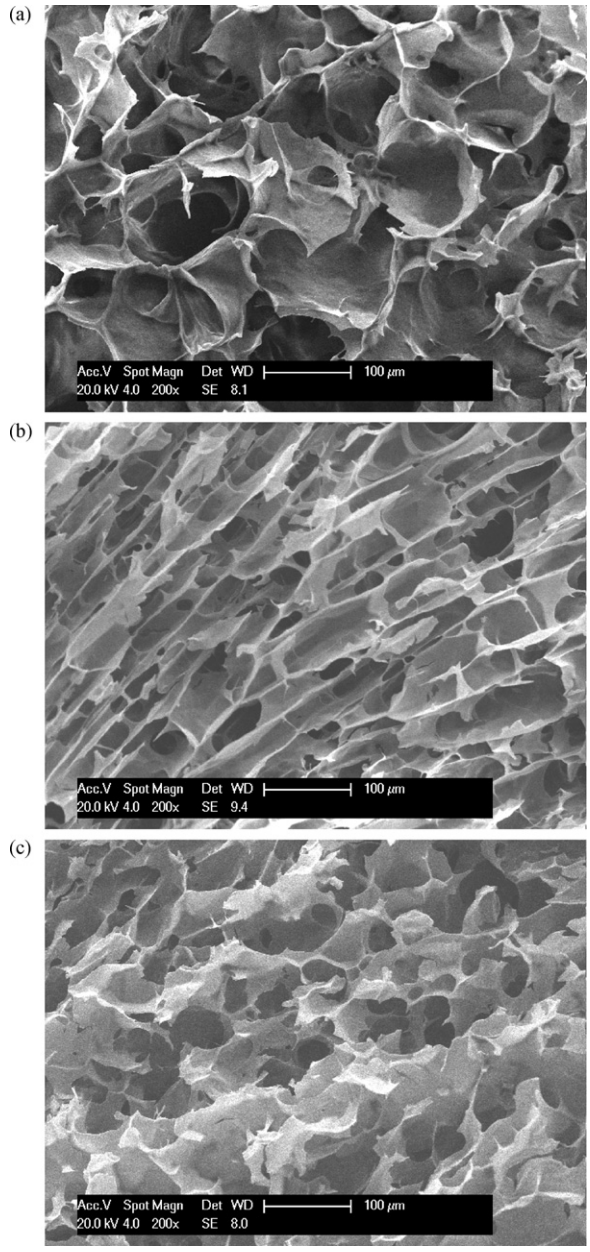

Fig. 4. SEM micrograph of the fractured surfaces of PS and SAPSs with different DSs (a, DS = 0; b, DS = 0.39; c, DS = 1.23).

appeared in the reaction of starch with octenyl succinic anhydride (Bhosale & Singhal, 2006). In addition, the maximum DS value (1.90) was observed at the SA/starch ratio of 1.5, while the maximum RE value (140.4%) was achieved at the SA/starch ratio of 1.2.

3.2. FTIR

The FTIR spectra of PS and SAPSs with different DSs are shown in Fig. 2. The band at about 3400 cm^{-1} was related to hydrogen-bonded hydroxyl groups of starch. In the fingerprint region of —C—O—C— stretching vibration in glucose bonds at 900–1200 cm^{-1}, the peak at about 1160 cm^{-1} was ascribed to C—O bond stretching of the C—O—H group, and the peaks at 1080 and 1020 cm^{-1} were attributed to C—O bond stretching of the C—O—C group in the anhydroglucose ring. Absorption bands due to C=O stretching of ester were observed at 1727 cm^{-1} in the SAPS (Yoshimura et al., 2006), and the peak at 1412 cm^{-1} corresponded to the carboxyl group of

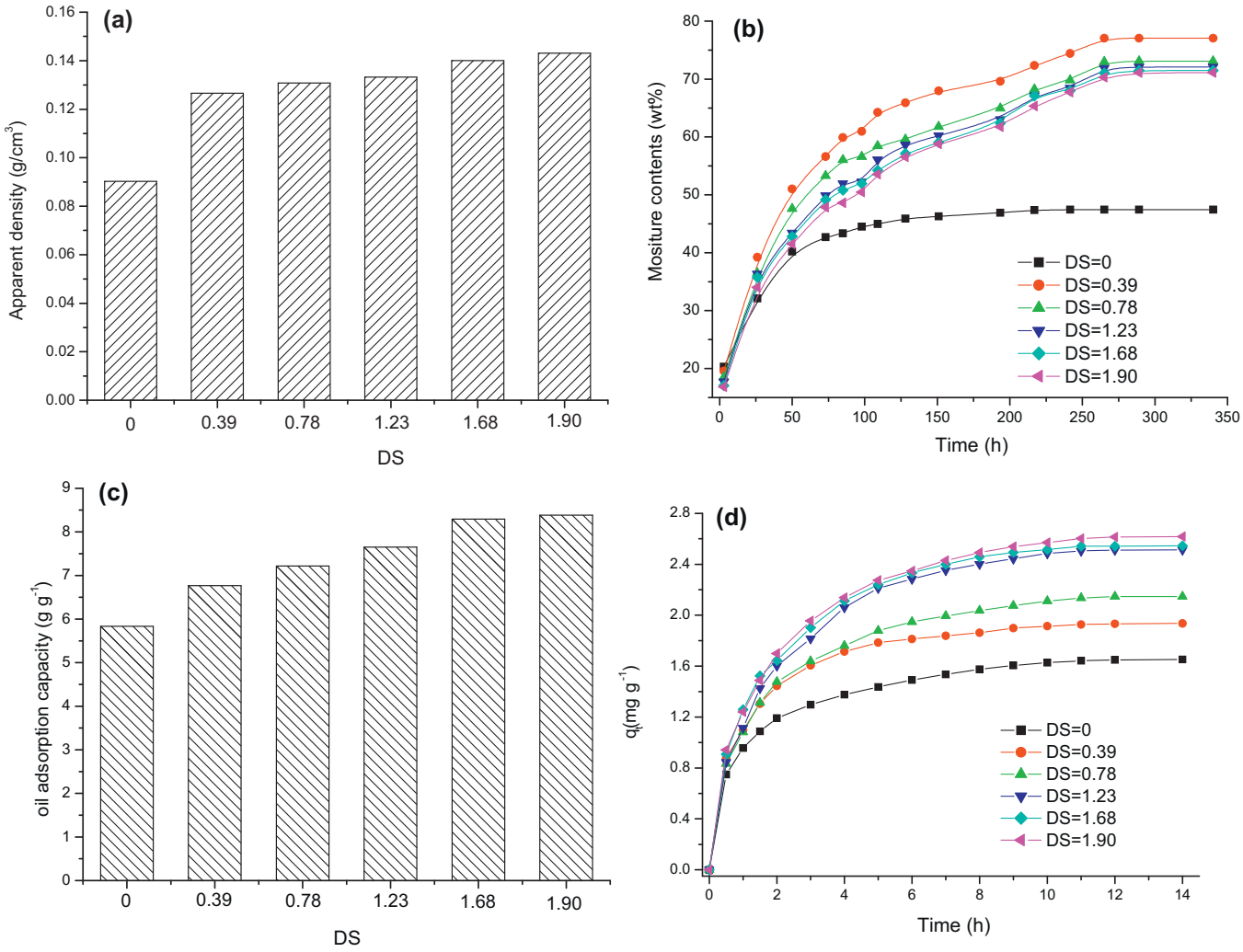

Fig. 5. Effect of different DSs (0–1.90) on the properties of SAPSs. (a) Apparent densities of SAPSs; (b) moisture absorption; (c) oil adsorption capacity; (d) MB adsorption. Initial concentration: MB 0.0854 mmol L^{-1} (31.93 mg L^{-1}) and SAPS 10 g L^{-1}.

the succinyl group (Huang, Bu, Jiang, & Zeng, 2011). These absorption bands were absent in PS which indicated the formation of esters by the reaction between the hydroxyl group in porous starch and the carboxylic anhydride group of SA. It was also observed that the intensity of these bands increased with the increasing DS values.

3.3. TG

The thermogravimetric (TG) and derivative thermogravimetric (DTG) curves of PS and SAPS powders are shown in Fig. 3. The decomposition temperature is the temperature at the maximum rate of mass loss, i.e. the peak temperature shown in DTG curves. The decomposition temperature of PS was 305 °C, while those of SAPS (DS = 0.39 and 1.68) were about 296 °C. SAPS exhibited lower thermal stability than PS, and the different DSs had little effect on that thermal stability. This could be attributed to the heating and denudation of starch during the esterification process, similar to the lower thermal stability of starch in starch–ZnO complex than raw starch (Ma, Chang, Yang, & Yu, 2009a).

3.4. SEM

Porous structures were obtained by substituting ice crystals in the frozen starch gel with ethanol using a solvent exchange technique. PS and SAPSs with different DSs are shown in Fig. 4. PS exhibited a pore size of about 100 μm, while the pore sizes of SAPS (DS = 0.39) and SAPS (DS = 1.23) were slightly reduced. And compared to PS, more opened pores were observed, which could come from reactive denudation during the reaction of SA with PS. Modification of SA could decrease the size of the holes, but there was no obvious difference among the morphologies of SAPSs with different DSs. Since the porous structures had formed before the modification of SA, the reactive heating process may shrink the pores and denude the walls of PS, but the different DSs could not change the pores.

3.5. Apparent density

Fig. 5a exhibits the dependence of apparent densities on DSs. The apparent density of PS was 0.09 g cm^{-3}. Compared to PS, the apparent densities of SAPS (DS = 0.39) was greatly enhanced to 0.127 g cm^{-3}, while the apparent densities of SAPSs only increased slightly, from 0.39 to 1.90, when the DSs increased. These results could be related to the morphology of SAPSs, as shown in Fig. 4. The modification of SA could decrease pore volumes and thereby improve the apparent densities. The different DSs had no obvious effect on pores sizes, so apparent densities changed very little.

Table 1
Adsorption kinetic constant of SAPSs (DS = 0–1.90) modeled by a pseudo second-order equation.

SAPS (DS)	T_{eq} (h)	$q_{e,exp}$ (mg g^{-1})	$q_{e,cal}$ (mg g^{-1})	k (mg g^{-1} h^{-1})	R
0	12	1.65	1.76	0.593	0.9992
0.39	12	1.93	2.07	0.582	0.9999
0.78	12	2.15	2.34	0.364	0.9996
1.23	12	2.51	2.84	0.239	0.9995
1.68	12	2.54	2.85	0.269	0.9996
1.90	12	2.61	2.91	0.254	0.9995

3.6. Moisture adsorption

Fig. 5b shows the effect of DS on the moisture absorption of SAPSs at 75% RH. It took about 150 h for PS to reach the moisture adsorption equilibrium, while more time (about 300 h) was required for SAPSs to reach equilibrium. Compared to PS (moisture content at equilibrium was 47.45%), SAPS exhibited higher moisture contents at equilibrium. This was attributed to the high water affinity brought along by the introduced carboxyl groups. However, when the DSs increased from 0.39 to 1.90, the moisture contents at equilibrium decreased somewhat, from 77.05% to 71.1%. In view of Eq. (3), the higher moisture adsorption could be counteracted by the increased weight of SAPS when more of the SAPS hydroxyl groups were substituted by SA.

3.7. Oil adsorption

The effect of different DSs on the oil adsorption capacity of SAPSs is illustrated in Fig. 5c. Although starch is hydrophilic by nature, PS showed a good capacity for oil adsorption, 5.84 g g^{-1} (oil/PS); this could be attributed to the porous structures which trapped and retained oil (Lawal & Adebowale, 2004). When the DSs increased, the oil adsorption capacity of SAPSs increased gradually because of more holes opening up. SAPS (DS = 1.90) exhibited an oil adsorption capacity of 8.39 g g^{-1} (oil/PS).

3.8. Adsorption of methylene blue (MB)

Fig. 5d shows the amounts of MB adsorbed by SAPSs of different DSs as a function of time. The amount of MB dye adsorbed at equilibrium by PS according to the experimental curves was 1.65 mg g^{-1}. When the DSs increased from 0.39 to 1.90, the amount of MB dye adsorbed at equilibrium increased from 1.93 to 2.61 mg g^{-1}. The newly grafted carboxylic groups brought negatively charged sorption sites that to some degree, formed an electrostatic attraction with the positively charged dye molecules (Huang et al., 2011). The adsorption behavior of SAPSs with different DSs (0–1.90) for MB can be described by a pseudo second-order model, expressed as Eq. (5):

$$\frac{t}{q_t} = \frac{1}{kq_e{}^2} + \frac{t}{q_e} \quad (5)$$

where k (mg g^{-1} h^{-1}) is the second-order rate constant, and q_t (mg g^{-1} PS) and q_e (mg g^{-1} PS) represent the amounts of dye adsorbed at any time t (h) and at equilibrium, respectively. The second-order rate constant k and q_e can be obtained from the intercept and slope of the line in a t/q_t versus t plot. Some kinetic parameters, estimated from the experimental data in Fig. 5d and using Eq. (5), are listed in Table 1. For the MB adsorption of SAPSs, linear relationships with high correlation coefficients ($R > 0.999$) between t/q_t and t indicate that the adsorption process could be described well by the pseudo second-order model.

4. Conclusion

Since starch granules and crystallinity are destroyed in starch gelatinization, large specific surface areas of PS thereby facilitated the modification reaction. The linear equation with a high correlation coefficient ($R > 0.99$) could be described as DS = 0.0224 + 1.3099 (molar ratio). SAPS exhibited lower thermal stability than PS, but the different DSs had little effect on the thermal stability of SAPSs. The reactive heating process shrank the pores and denuded the walls of PS, but improved the apparent densities. SAPS exhibited higher moisture contents at equilibrium than PS. With the increasing of DSs, the oil adsorption capacity and MB adsorption of SAPSs increased gradually. And the MB adsorption process could be described well by a pseudo second-order model. SAPS can extend the further application of PS in food, pharmaceuticals, agriculture, cosmetics, pulp and paper, and other industries.

References

Aburto, J., Alric, I., & Borredon, E. (2005). Organic solvent-free transesterification of various starches with lauric acid methyl ester and triacyl glycerides. *Starch/Stärke*, *57*, 145–152.

Bai, Y. J., & Shi, Y. C. (2011). Structure and preparation of octenyl succinic esters of granular starch, microporous starch and soluble maltodextrin. *Carbohydrate Polymers*, *83*, 520–527.

Bhosale, R., & Singhal, R. (2006). Process optimization for the synthesis of octenyl succinyl derivative of waxy corn and amaranth starches. *Carbohydrate Polymers*, *66*, 521–527.

Chang, P. R., Yu, J. G., & Ma, X. F. (2011). Preparation of porous starch and its use as a structure-directing agent for production of porous zinc oxide. *Carbohydrate Polymers*, *83*, 1016–1019.

Huang, X. Y., Bu, H. T., Jiang, G. B., & Zeng, M. H. (2011). Cross-linked succinyl chitosan as an adsorbent for the removal of Methylene Blue from aqueous solution. *International Journal of Biological Macromolecules*, *49*, 643–651.

Lawal, O. S., & Adebowale, K. O. (2004). Effect of acetylation and succinylation on solubility profile, water absorption capacity, oil absorption capacity and emulsifying properties of mucuna bean (Mucuna pruriens) protein concentrate. *Nahrung/Food*, *48*, 129–136.

Ma, X. F., Chang, P. R., Yang, J. W., & Yu, J. G. (2009). Preparation and properties of glycerol plasticized-pea starch/zinc oxide-starch bionanocomposites. *Carbohydrate Polymers*, *75*, 472–478.

Ma, X. F., Chang, P. R., Yu, J. G., & Stumborg, M. (2009). Properties of biodegradable citric acid-modified granular starch/thermoplastic pea starch composites. *Carbohydrate Polymers*, *75*, 1–8.

Ma, X. F., Jian, R. J., Chang, P. R., & Yu, J. G. (2008). Fabrication and characterization of citric acid-modified starch nanoparticles/plasticized–starch composites. *Biomacromolecules*, *9*, 3314–3320.

Qian, D. Y., Chang, P. R., & Ma, X. F. (2011). Preparation of controllable porous starch with different starch concentrations by the single or dual freezing process. *Carbohydrate Polymers*, *86*, 1181–1186.

Shogren, R. L. (2003). Rapid preparation of starch esters by high temperature/pressure reaction. *Carbohydrate Polymers*, *52*, 319–326.

Wang, X. Y., Li, X. X., Chen, L., Xie, F. W., Yu, L., & Li, B. (2011). Preparation and characterisation of octenyl succinate starch as a delivery carrier for bioactive food components. *Food Chemistry*, *126*, 1218–1225.

Wong, A., Chu, R. K. M., Leung, S. N., Park, C. B., & Zong, J. H. (2011). A batch foaming visualization system with extensional stress-inducing ability. *Chemical Engineering Science*, *66*, 55–63.

Yoshimura, T., Yoshimura, R., Seki, C., & Fujioka, R. (2006). Synthesis and characterization of biodegradable hydrogels based on starch and succinic anhydride. *Carbohydrate Polymers*, *64*, 345–349.